Article https://www.korseaj.org

Vision-Based Smart Beehive Integrating Environmental Sensing for Climate-Smart Apiculture

Taehyun Kim [1], Kyeong Yong Lee [2], Jeongwook Heo [1], Jeonghyun Baek [1], Jeongho Lee [1] and Hyeonbyeong Lee [3*]

[1]Smart Farm Development Department, Agricultural Engineering Division, National Institute of Agricultural Sciences, Rural Development Administration, Wanju 55365, Korea, [2]Apiculture Department, Agricultural Biology Division, National Institute of Agricultural Sciences, Rural Development Administration, Wanju 55365, Korea, [3]Department of Computer Engineering, Dorim Campus, Mokpo National University, Muan 58554, Korea
* Corresponding author: Hyeonbyeong Lee

Abstract: This study presents a field-deployable smart beehive that combines real-time, vision-based in/out counting with continuous environmental sensing on low-power edge hardware. A four-zone entrance model with a conservation constraint ($\Delta A = 0$) is introduced to regularize event inference, and practical stabilizers—a boundary buffer, short debouncing, and per-track cooldown—are used to suppress spurious transitions caused by jitter, occlusion, and brief reversals on the entrance lip. The system runs on a Raspberry Pi with an optional Edge TPU accelerator and exposes a dashboard that collocates entrance activity with internal and external temperature, humidity, CO_2, and hive weight for management decisions. Field experiments at two outdoor sites show that the proposed Algorithm 2 achieves event-level IN accuracy of 82.8–88.2% and OUT accuracy of 97.1–100.0%, substantially reducing double counts relative to an aggregate-zone baseline while maintaining real-time performance on embedded hardware. By interpreting the joint activity and microclimate time series in the context of climate-smart agriculture, precision apiculture, and agricultural-environment indicators, we demonstrate how the smart beehive can function not only as an automated counter, but also as a sensor node for pollinator-aware, climate-smart farm management.

Keywords: *Apis mellifera*, Climate-smart agriculture, Computer vision, Environmental monitoring, Precision apiculture, Smart beehive

https://doi.org/10.5338/KJEA.2025.44.44

Agric. Environ. Sci. 2025, 44, 462-473

Received: November 20, 2025
Revised: November 25, 2025
Accepted: December 1, 2025
Published: December 8, 2025

Online ISSN: 2233-4173
Print ISSN: 1225-3537

Check for updates

Introduction

Honey bees are central to agricultural productivity and ecosystem services, and their foraging activity reflects short-term colony condition as well as landscape resource availability [1–3]. Reliable, scalable measurement of entrance traffic therefore offers practical indicators for agricultural and apicultural management. Traditional approaches—manual tallying, infrared (IR) beam gates, or tag-based systems—face important limitations: manual counts do not scale and are observer-dependent; IR beams suffer from occlusion and bidirectional interference during congested flows; and tags or markers increase cost and alter natural behavior, constraining field deployment [4–6].

Computer-vision methods have emerged as a non-intrusive alternative. Early systems relied on background subtraction and blob heuristics, which degrade under illumination changes, moving shadows, and overlapping bodies near hive slits. Recent object-detection pipelines and tracking-by-detection strategies improve robustness but remain challenged by (i) frequent direction reversals and short loitering bouts on the entrance lip, (ii) heavy occlusion in peak periods, and (iii) the compute and memory constraints of low-power edge devices used in outdoor apiaries [7–9]. As a result, over-counting (double counts) and direction flips are common failure modes, especially when frame rate is low or boundary definitions are tight. Recent work using on-hive video loggers has also explored accuracy–energy trade-offs for bee object detection using YOLO variants [10].

This work develops a field-deployable smart beehive that integrates environmental sensing with real-time, vision-based counting on frugal hardware. We formalize a four-zone entrance model with a conservation constraint ($\Delta A = 0$) to regularize event inference and introduce practical stabilizers—a boundary buffer, short debouncing, and cooldown—to suppress spurious transitions caused by jitter and brief reversals. The system runs on a Raspberry Pi with an optional Edge TPU accelerator and exposes a dashboard that collocates IN/OUT time series with internal and external temperature and humidity, CO_2, and hive weight for management decisions.

From the perspective of environmental agriculture, climate-smart agriculture (CSA) frameworks emphasize the joint goals of sustaining productivity, enhancing resilience to climate variability, and reducing greenhouse-gas emissions. Recent CSA-based assessments of rice systems in Korea illustrate how weather variability, yield, and methane emissions trade off at the field scale [11]. Similar climate-driven stressors act on pollinators: extreme heat, unseasonal warm spells, and prolonged drought can disrupt floral resources and increase the thermoregulatory load on colonies. A smart beehive that records hive microclimate together with entrance activity can therefore function as a CSA adaptation tool that helps maintain pollination services under changing climatic conditions.

Smart-farm and smart-greenhouse infrastructures already use networked sensors, actuators, and cloud-based data analysis to manage nutrient solutions and environmental parameters in controlled-environment agriculture [12,13]. At the same time, honey bees and bumblebees remain highly sensitive to agricultural chemicals such as neonicotinoid insecticides and to broader environmental quality, which is increasingly monitored through agricultural-environment conservation programs and air-quality networks [14–16]. At a broader information-systems level, large-scale log-analysis infrastructures such as Beehive [17] illustrate how heterogeneous telemetry can be mined for incident detection. In parallel, precision-beekeeping surveys and systematic reviews report a strong trend toward intelligent, data-driven hive monitoring, encompassing environmental, acoustic, and visual sensing modalities and a variety of analytical services to support colony management [18–20]. Positioning our system within this landscape, we view the proposed smart beehive not only as a counting device but also as a sensor node that can feed into climate-smart, pollinator-aware farm management.

Continuous monitoring of hive weight, temperature, and other physical variables has been used to characterize colony phenology, foraging dynamics, and responses to environmental conditions without intrusive inspections [21–23]. Wireless sensor networks and Internet-of-Things (IoT) architectures for precision apiculture extend this approach by distributing sensor nodes across many hives and sites, supporting remote observation and early-warning services [24–26]. Concurrently, studies of honey bee thermal homeostasis and heat-stress responses have highlighted the narrow temperature range required for brood development and the colony-level behaviors that emerge to buffer against heat and cold [27,28]. These biological insights motivate the integration of entrance activity and microclimate telemetry—here meaning continuous measurements of internal hive temperature, relative humidity, CO_2 concentration, and hive weight—together with embedded analytics into a single platform that can support both engineering and ecological interpretations of hive status.

This work makes three main contributions. First, we design and implement a vision-based smart beehive that combines entrance video, environmental sensing, and an embedded dashboard on a low-power edge device suitable for deployment in real apiaries. Second, we propose a conservation-aware four-zone entrance model with lightweight temporal stabilizers—where "conservation-aware" indicates that the total number of bees in the global entrance set is constrained to be conserved ($\Delta A =$

0) between consecutive frames—and systematically analyze how frame rate and boundary spacing affect IN/OUT counting accuracy in field conditions. Third, we interpret the joint activity and environmental time series within climate-smart agriculture, smart-farm, and environmental-indicator frameworks, relating hive-level signals to broader agricultural-environment contexts and pollinator biology.

Results and Discussion

Counting accuracy of the four-zone model

Event-level accuracy for the proposed method (Algorithm 2) was as follows: Site 1 — IN ≈ 82.8%, OUT ≈ 97.1%; Site 2 — IN ≈ 88.2%, OUT ≈ 100.0%. Environment-wise summary accuracies are provided in Fig. 1a (IN) and Fig. 1b (OUT), and minute-level trajectories for each environment–algorithm pair appear in Fig. 2a–d. Table 1 further summarizes IN and OUT accuracies together with the net count error (predicted minus ground-truth events) for each algorithm–site pair; positive error values indicate net over-counting and negative values net under-counting relative to ground truth. This tabular view makes it visually clear that the aggregate-zone baseline (Algorithm 1) strongly over-counted both IN and OUT events, whereas the conservation-aware four-zone formulation (Algorithm 2) remained nearly unbiased, with only small residual count errors. Compared with Algorithm 1, Algorithm 2 thus markedly reduced over-counting from brief oscillations, with residual discrepancies concentrated in a small number of ambiguous or congested intervals. These results indicate that the conservation-aware four-zone formulation can deliver stable counting performance under realistic outdoor conditions while keeping the event logic lightweight enough for embedded deployment (see Counting Algorithms in Materials and Methods for implementation details).

Across both sites, the CPU-only pipeline sustained approximately 3–4 frames per second (fps), whereas the Edge TPU config-

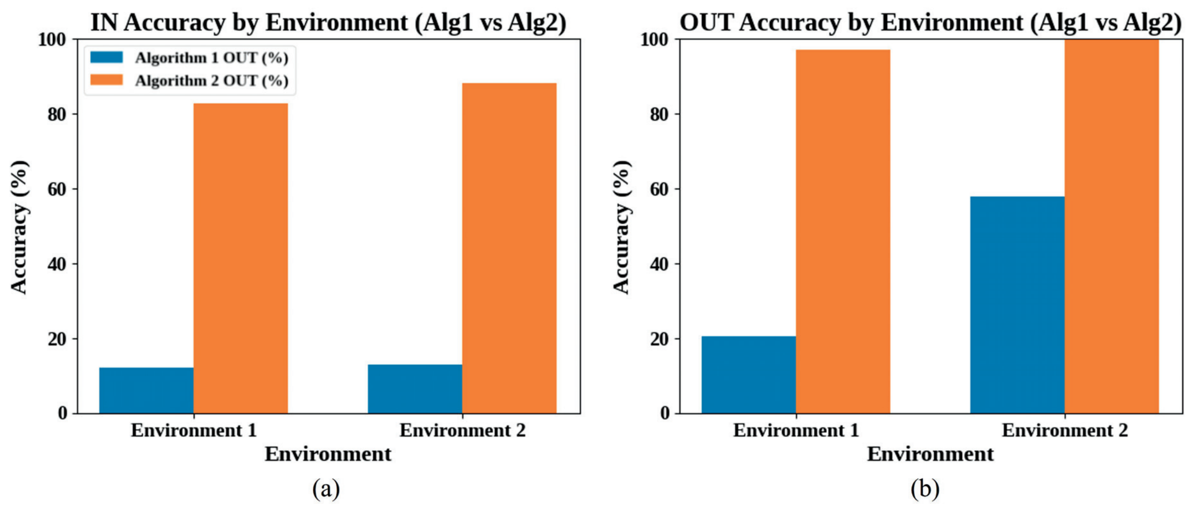

Fig. 1. Summary accuracies by environment and algorithm: (a) IN accuracy; (b) OUT accuracy (Algorithm 1 vs. Algorithm 2).

Table 1. Summary IN and OUT accuracies and total count errors for each algorithm and site (positive error values indicate net over-counting and negative values net under-counting relative to ground truth)

Environment	Algorithm	IN accuracy (%)	OUT accuracy (%)	IN total count error (pred – gt)	OUT total count error (pred – gt)
Environment 1	Algorithm 1	12.0	20.4	+221	+90
	Algorithm 2	82.8	97.1	+5	−1
Environment 2	Algorithm 1	12.8	57.7	+136	+22
	Algorithm 2	88.2	100.0	+2	0

https://doi.org/10.5338/KJEA.2025.44.44
Agric. Environ. Sci. 2025, 44, 462-473

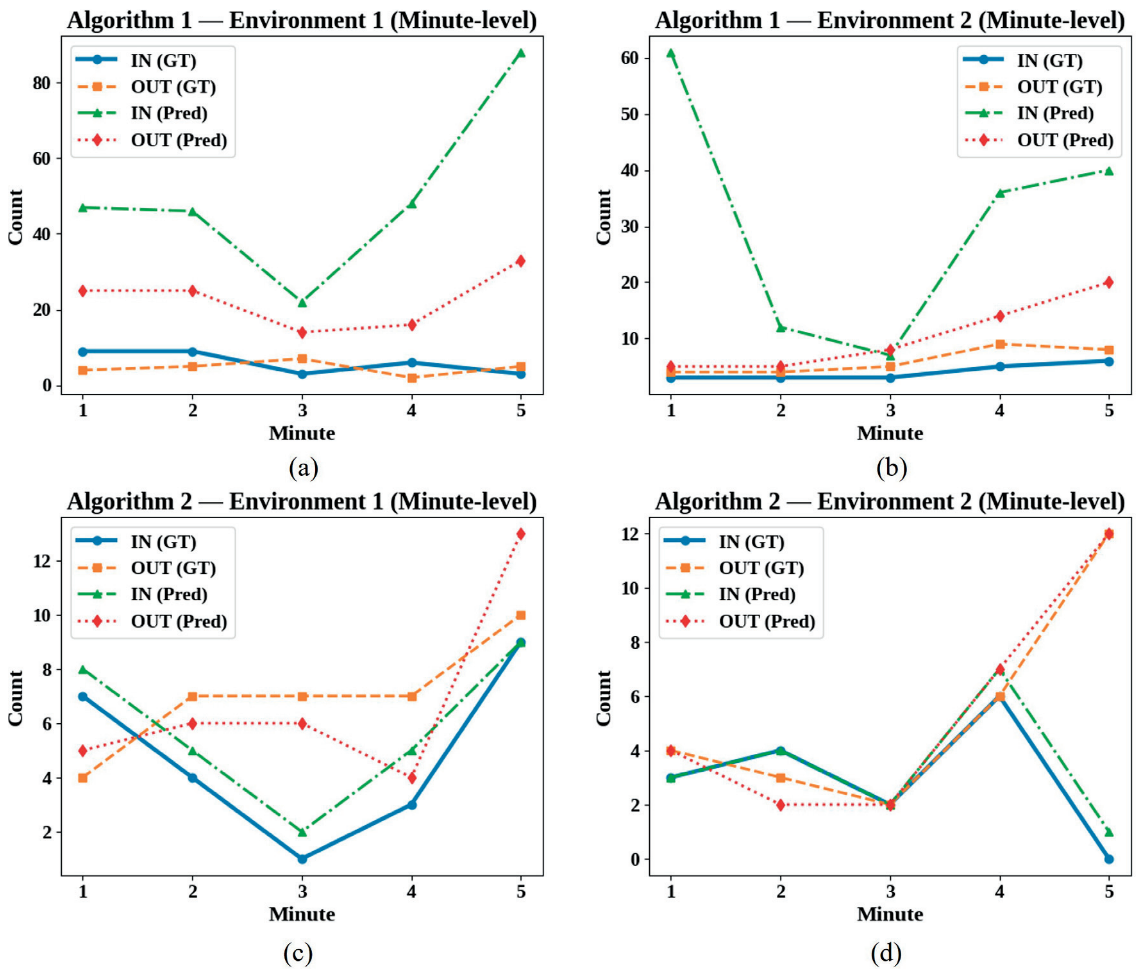

Fig. 2. Minute-level ground-truth and predicted counts: (a) Algorithm 1 — Environment 1; (b) Algorithm 1 — Environment 2; (c) Algorithm 2 — Environment 1; (d) Algorithm 2 — Environment 2.

uration sustained approximately 25–30 fps on the same scenes. End-to-end latency (capture → detection → association → event logic → user interface) remained under 1 s with the accelerator even with debouncing and cooldown enabled, while CPU-only operation frequently exceeded this during bursts of activity. Higher fps yielded longer track lifetimes and fewer frame-to-frame zone oscillations, particularly in congested entrance conditions. Detector performance was robust to moderate illumination change, moving vegetation, and partial occlusions at the slit. False positives were most common on specular highlights and stationary debris. Prolonged presence at the lip could mask true crossings; the proposed Algorithm 2 mitigated this via conservation ($\Delta A = 0$), boundary buffers, and short temporal persistence before committing events. Physical boundary spacing and frame rate jointly affected accuracy. A spacing of approximately 3 cm or more at ≥25 fps reduced oscillation-induced reversals and stabilized inference; tighter spacing (approximately 1–2 cm) increased spurious transitions, particularly on CPU where low fps magnified inter-frame displacement. The dashboard co-visualized IN/OUT counts, fps, and environmental telemetry (internal and external temperature and humidity, CO_2, and hive weight), supporting interpretation of midday ventilation and transient slowdowns. We note several limitations of the present field validation. First, the two outdoor sites used in this study represented temperate conditions without prolonged periods of heavy rain or strong winds, and we did not systematically test performance under very low-light levels at dawn, dusk, or heavily overcast days. Under such conditions, detection performance may degrade unless additional measures such as infrared illumination, more aggressive exposure control, or higher-sensitivity cameras are employed. Second, although the four-zone entrance model and stabilizers were designed to be robust under congested entrance conditions, extremely dense traffic periods in which the slit is continuously blocked by overlapping bodies can still lead to under-counting or delayed event confirmation

https://doi.org/10.5338/KJEA.2025.44.44
Agric. Environ. Sci. 2025, 44, 462-473

because individual bees cannot be reliably separated. Third, environmental factors such as water droplets, condensation, or debris on the camera window during adverse weather can temporarily obscure the entrance region and cause intermittent loss of detections until maintenance is performed. Future work will therefore include longer-term, multi-season deployments at additional sites to quantify system performance across a wider range of climatic conditions, beekeeping practices, and entrance congestion levels.

Colony activity and microclimate regulation

From a biological perspective, the combined IN/OUT trajectories and microclimate telemetry provide more than simple traffic counts. Daily activity profiles showed characteristic morning ramp-up and evening decline, with superimposed short-term fluctuations that likely reflect changes in forage availability and weather. Such patterns are consistent with previous work using continuous hive weight and environmental measurements to infer foraging dynamics and colony phenology [21–23]. Networks of smart beehives deployed across agricultural landscapes could therefore serve as distributed sensors of phenological shifts, forage dearths, or stress events that affect many colonies simultaneously.

Microclimate measurements from the smart beehive also shed light on colony-level thermal homeostasis. Internal temperature remained within a relatively narrow band compared with external temperature, despite substantial diurnal swings outside the hive, and short bursts of entrance activity coincided with CO_2 peaks and subsequent declines, suggesting coordinated ventilation. Representative multi-day trajectories combining entrance counts with internal and external temperature, humidity, and CO_2 illustrate how colonies adjust activity and ventilation under varying ambient conditions (Fig. 3). These observations align with experimental studies showing that honey bee colonies employ water cooling, fanning, and redistribution of workers to maintain brood temperatures in the biologically preferred range and to respond to heat stress [27,28]. Comparisons of internal hive temperature between conventional and smart hives under similar outdoor conditions (Fig. 4) further emphasize the potential of active

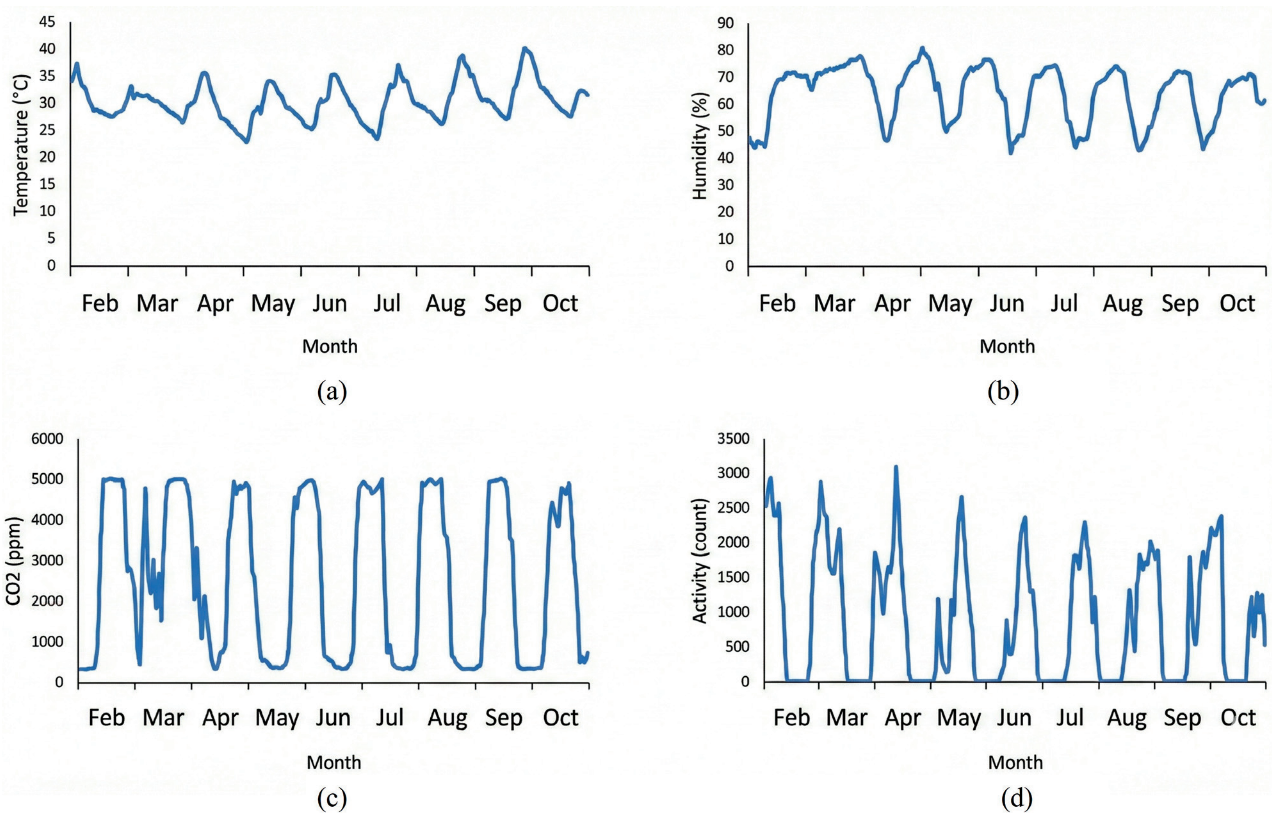

Fig. 3. Representative multi-day trajectories of entrance activity and hive microclimate: (a) internal and external temperature; (b) internal relative humidity; (c) internal CO_2 concentration; (d) IN/OUT counts per minute.

https://doi.org/10.5338/KJEA.2025.44.44
Agric. Environ. Sci. 2025, 44, 462-473

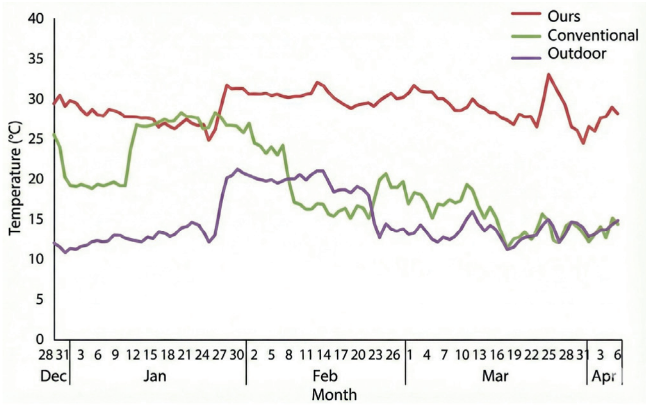

(a)

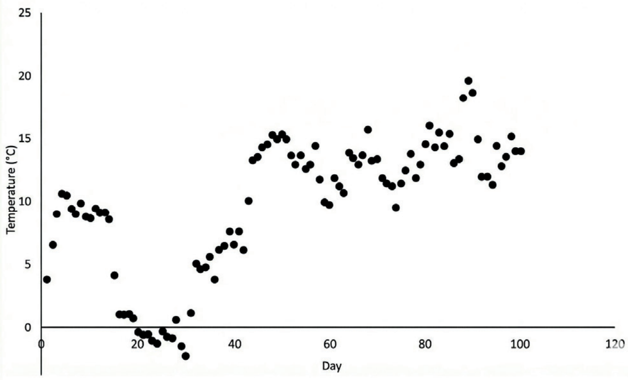

(b)

Fig. 4. Comparison of internal hive temperature under conventional and smart hives: (a) internal temperature time series for conventional vs. smart hives under similar outdoor conditions; (b) distribution of daily minimum and maximum temperatures highlighting improved thermal buffering in the smart beehive.

microclimate management to buffer colonies against thermal extremes.

Greenhouse case study and environmental-agriculture implications

In a pilot deployment in a commercial tomato greenhouse in Goheung, we further examined how entrance activity relates to hive microclimate and crop production. Table 2 summarizes Pearson correlation coefficients between bee activity and mean sensor values at different aggregation windows (12 h, 24 h, 1 week, and 1 month), as well as the correlation between monthly cumulative bee activity and tomato yield. Short-term windows showed modest correlations between activity and internal temperature or CO_2, whereas weekly and monthly aggregations exhibited stronger positive associations (up to r = 0.90 for internal temperature and r = 0.62 for CO_2), reflecting that periods of sustained foraging and ventilation coincide with elevated internal temperature and metabolic CO_2 loads. Monthly cumulative bee activity displayed a very strong correlation with harvested tomato yield (r = 0.95; $r^2 \approx 0.90$), indicating that months with higher cumulative activity tended to coincide with higher tomato production during the observation period. However, this estimate is based on a limited number of monthly observations collected from a single commercial greenhouse during one cultivation cycle, and other management factors (e.g., cultivar, climate-control setpoints, nutrient regime, and colony strength) were not controlled experimentally. We therefore regard this correlation as a preliminary, site-specific observation rather than strict evidence of a causal relationship between bee activity and tomato yield.

At larger spatial scales, networks of such smart beehives deployed across agricultural landscapes could contribute to quantitative assessments of agricultural-environment quality. Because bees forage over wide areas and respond to pesticide exposure, air-pollutant loads, and broader agricultural-environment conditions [14–16], deviations in entrance activity or hive condition shared by many colonies may signal wider environmental problems. This aligns with the broader use of indicators in agricultural-environment conservation programs and with recent developments in precision apiculture and smart-beehive technologies

Table 2. Pearson correlation coefficients between bee activity and mean sensor values at different aggregation windows in a commercial tomato greenhouse and between monthly cumulative bee activity and tomato yield

Aggregation window	Internal temperature	External temperature	Relative humidity	CO_2 concentration	Tomato yield
12 h	0.31	-0.014	0.12	0.099	–
24 h	0.25	0.22	-0.051	0.10	–
1 week	0.42	0.22	0.011	0.21	–
1 month	0.90	-0.037	-0.11	0.62	0.95

https://doi.org/10.5338/KJEA.2025.44.44
Agric. Environ. Sci. 2025, 44, 462-473

[18–20,24–26]. By analogy with large-scale log-analysis infrastructures in enterprise networks [17], future smart-apiculture systems will likely need to aggregate heterogeneous data streams from many hives and farms, using analytics informed by both engineering performance and biological responses to prioritize incidents and support decision-making.

A conservation-aware four-zone model, coupled with lightweight temporal stabilizers, yields stable IN/OUT counts on low-power hardware. Across two outdoor sites, the system achieved event-level IN accuracy of 82.8–88.2% and OUT accuracy of 97.1–100.0%, with best performance under higher frame rates and adequate boundary spacing. Relative to aggregate-zone methods, the approach substantially reduced double counts caused by brief reversals and boundary jitter, providing a pragmatic basis for routine hive-activity monitoring. These findings should be interpreted in light of the fact that our field tests covered only two sites and a limited range of weather and lighting conditions; broader, multi-season deployments under more extreme low-light, adverse-weather, and highly congested entrance scenarios will be necessary to fully characterize system performance.

Beyond its technical performance, the smart beehive developed in this study links smart apiculture to the broader goals of environmental agriculture. By continuously recording entrance activity together with hive microclimate and weight, the system can support climate-smart beekeeping practices, contribute to smart-farm monitoring architectures, and provide bioindicator signals relevant to agricultural-environment conservation and air-quality management [11–16,18–20,21–28]. Future work includes seasonal and multi-site deployments, applications in pesticide and environmental-risk assessment, and integration of hive-activity indicators with crop performance and ecosystem-service metrics.

Materials and Methods

The platform used a Raspberry Pi 4B (5 V / 4 A) with an optional Coral Edge TPU accelerator. Environmental context was captured via internal and external temperature and humidity sensors (e.g., SHT30, DHT22), a nondispersive infrared CO_2 sensor (e.g., CM1107), and a load cell for hive-weight monitoring (e.g., CZL635, 5 kg). Optional relays drove a heater and cooling fan. A web or on-screen dashboard presented IN/OUT counts, frames per second (fps), environmental time series, network status, and date and time. The detailed hardware and sensor specifications are summarized in Table 3, and the physical enclosure, sensor module, and I/O layout are illustrated in Fig. 5.

A fixed camera was mounted approximately orthogonal to the entrance plane, with a small ruler near the slit to enable pixel–centimeter conversion. Representative camera views for long-range capture of honey bee (Apis mellifera) colonies at outdoor hives and close-range capture of bumblebee (Bombus spp.) colonies in greenhouse pollination hives are also shown in Fig. 5. The entrance model comprised four zones—A (global), B (inside), C (outside), and D (edge buffer). Inter-boundary spacing between B–C and C–D was set to approximately 3 cm at ≥25 fps to reduce rapid state thrashing. For each site, camera intrinsics and extrinsics, the entrance region-of-interest (ROI) mask, and boundary coordinates were stored. An example on-screen overlay with the four-zone layout, entrance ROI, zone counters (A–D), frame rate, and environmental telemetry is displayed on the

Table 3. Hardware and sensor specifications for the smart beehive platform

Component	Model/Part	Specifications/Notes
Raspberry Pi 4B		5 V / 4 A power supply
Edge TPU (USB)		Optional accelerator
Temp/Humidity Sensor	SHT30 / DHT22	Internal / external
CO_2 Sensor	CM1107 (example)	
Load Cell	CZL635 (5 kg)	
Relay Module		Heater / Fan control
Camera		Entrance slit coverage; include ruler

https://doi.org/10.5338/KJEA.2025.44.44
Agric. Environ. Sci. 2025, 44, 462-473

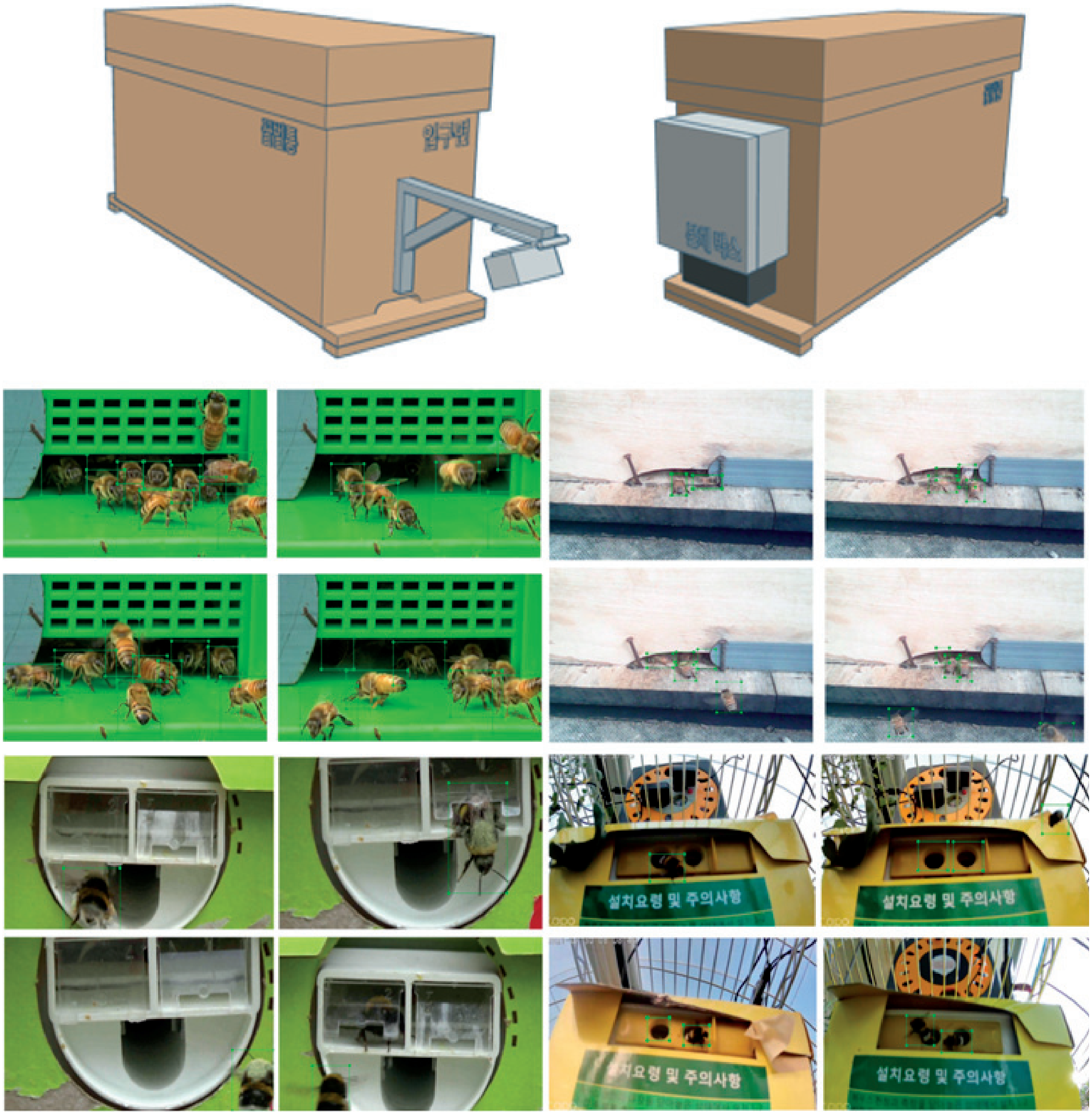

Fig. 5. Smart beehive hardware and entrance views in the experimental environments: top—schematic enclosures and sensor modules for the honey bee (*Apis mellifera*) and bumblebee (*Bombus* spp.) hives; middle—example long-range entrance views for honey bee colonies at outdoor hives; bottom—example close-range entrance views for bumblebee colonies in greenhouse pollination hives.

dashboard.

Object detection (training classes)

A lightweight single-shot detector (MobileNet-SSD variant) was trained with three classes: Honeybee (Apis mellifera), Bumblebee (Bombus spp.), and Entrance (gate or slit). Data augmentation (rotation, scale, translation, and illumination jitter) increased robustness to field variability. Inference ran on the CPU (approximately 3–4 fps) or the Edge TPU (approximately 25–30 fps). Confidence and non-maximum suppression thresholds were tuned per lighting condition, and detections were filtered by the ROI before being passed to the counting logic. The detector was initialized from a publicly available MobileNet-SSD checkpoint and fine-tuned on several thousand annotated entrance frames extracted from our field videos. Frames were split into training and validation subsets (approximately 80:20) on a hive-by-hive basis to reduce leakage. Training used a modern deep-learning framework with an Adam optimizer (initial learning rate on the order of 10^{-4}, mini-batch size 32) for up to 50

https://doi.org/10.5338/KJEA.2025.44.44
Agric. Environ. Sci. 2025, 44, 462-473

epochs, with early stopping based on validation loss. Model weights and configuration files were kept fixed for all experiments reported in this study.

Counting algorithms

At a high level, both Algorithm 1 and Algorithm 2 follow the same processing pipeline: per-frame detection of bees and the entrance, assignment of detections to predefined entrance zones, computation of zone-wise count changes between consecutive frames, and simple rule-based inference of IN/OUT events from those changes. Two formulations were implemented. The baseline Algorithm 1 aggregates population changes in zones B and C without a conservation constraint. After per-frame detection and counting of (nA, nB, nC), frame-to-frame deltas (dA, dB, dC) are computed and, when a short debouncing window holds, entries are inferred when dC < 0 and dB > 0 and exits when dB < 0 and dC > 0, incremented by min(|dC|, dB) or min(|dB|, dC). This method is responsive but sensitive to lip loitering and boundary jitter because partial cancellations are not enforced (Fig. 6). In our implementation, the inner and outer entrance boundaries (between B and C, and between C and D) were spaced by approximately 3 cm, and the minimum-displacement threshold min_gap was set to roughly one third of this spacing in image-space pixels. The boundary buffer was set to ±2 pixels and the debouncing window to 3 consecutive frames, while the per-track cooldown was set to 0.5 s. These values were chosen empirically based on preliminary trials and then held fixed for both environments; they can be adjusted in software to accommodate different camera geometries or entrance sizes.

Algorithm 1: Baseline In/Out Counting (3-zone, no conservation)

```
Require: frames, regions(A,B,C), τ, W
Ensure: IN, OUT
IN, OUT ← 0, 0;  init ← false
for each f in frames do
    det ← DETECT(f, τ)
    (nA, nB, nC) ← COUNT(det, regions)
    if init then
        (dA, dB, dC) ← (nA, nB, nC) − (nA_0, nB_0, nC_0)
        if DEBOUNCE(W) then
            if (dC < 0) and (dB > 0) then                    ▷ C↓, B↑ ⇒ IN
                IN ← IN + min(|dC|, dB)
            else if (dB < 0) and (dC > 0) then               ▷ B↓, C↑ ⇒ OUT
                OUT ← OUT + min(|dB|, dC)
            end if
        end if
    end if
    (nA_0, nB_0, nC_0, det_0, init) ← (nA, nB, nC, det, true)
end for
return (IN, OUT)
```

Fig. 6. Baseline Algorithm 1 (three-zone aggregate) for IN/OUT event inference.

The schematic summarizes the main steps of the baseline pipeline: object detection and region-of-interest filtering, aggregate zone counting, computation of frame-to-frame zone-count deltas, and simple debounced logic for committing IN and OUT events.

The proposed Algorithm 2 introduces a four-zone layout (A/B/C/D) and enforces conservation of the global set (ΔA = 0). Events are confirmed only for true traversals: C→B is counted as IN; B→C as OUT; and C→D as OUT (departure). D→C cancels a pending OUT and B→D is treated as a non-event. Stabilizers include a ±1–2 pixel boundary buffer, 2–3 frame debouncing, a short per-track cooldown (hundreds of milliseconds), a minimum-displacement check Crossed(·) ≥ min_gap, and a short-track merge heuristic (Fig. 7).

Algorithm 2: In/Out Counting (4-zone, conservation-aware)

Require: frames, regions, τ, W, T_{block}, min_gap
Ensure: IN, OUT

```
IN, OUT ← 0, 0;  init ← false
for each f in frames do
    det ← DETECT(f, τ)
    (nA, nB, nC, nD) ← COUNT(det, regions)
    if init then
        (dA, dB, dC, dD) ← (nA, nB, nC, nD) − (nA0, nB0, nC0, nD0)
        if dA = 0 and DEBOUNCE(W) and COOLDOWN(T_block) then
            if (nC0 > nC) and (nB > nB0) and CROSSED(C→B, det0, det, min_gap) then
                IN ← IN + 1
            else if (nC0 > nC) and (nD > nD0) and CROSSED(C→D, det0, det, min_gap) then
                OUT ← OUT + 1
            end if
        end if
        (nA0, nB0, nC0, nD0, det0, init) ← (nA, nB, nC, nD, det, true)

        return (IN, OUT)
```

Fig. 7. Proposed Algorithm 2 (four-zone with conservation) for IN/OUT event inference with debouncing, cooldown, and minimum-displacement checks.

The schematic highlights the conservation-aware four-zone model with temporal stabilizers, including a global conservation constraint on the entrance set ($\Delta A = 0$), a short per-track cooldown, 2–3 frame debouncing, minimum-displacement checks, and a short-track merge heuristic.

Two outdoor sites representing different entrance congestion levels and background clutter were used. At each site, a 5-min clip was annotated to produce frame-accurate IN and OUT event lists; slow-motion adjudication was used for ambiguous sequences. Primary metrics were event-level accuracy for IN and OUT. We report means ± standard deviations and Wilson 95% confidence intervals; where appropriate, paired comparisons (for example, CPU vs. TPU on identical clips) used two-sided tests with $\alpha = 0.05$.

Implementation details

All processing was implemented in Python on Raspberry Pi OS, using OpenCV for video capture and pre-processing and a TensorFlow Lite–based runtime for MobileNet-SSD inference, with optional Coral Edge TPU acceleration. Event and sensor time series were stored locally in a lightweight database and exposed through a simple web server for real-time visualization on the integrated dashboard or remote clients.

Data Availability: All data are available in the main text or in the Supplementary Information.

Author Contributions: T.K. conceived and designed the research; T.K., K.L., J.H., J.B. and J.L. collected the data and performed the analysis; T.K. and K.L. wrote the first draft of the manuscript; J.H., J.B., J.L. and H.L. revised the manuscript. All authors have read and agreed to the published version of the manuscript.

Notes: The authors declare no conflict of interest

Acknowledgments: The author(s) declare that financial support was received for the research and/or publication of this article.

This work was supported by a research program of the Rural Development Administration (Project No. PJ01595302), Republic of Korea. We also acknowledge the technical support provided by staff at the National Institute of Agricultural Sciences for their contributions to system construction and maintenance.

Additional Information:

Supplementary information The online version contains supplementary material available at https://doi.org/10.5338/KJEA.2025.44.44

Correspondence and requests for materials should be addressed to Hyeonbyeong Lee.

Peer review information Agricultural and Environmental Sciences thanks the anonymous reviewers for their contribution to the peer review of this work.

Reprints and permissions information is available at http://www.korseaj.org

References

1. Son JD, Lim S, Kim D, Han G, Ilyasov R, Yunusbaev U, Kwon HW (2019) Automatic bee-counting system with dual infrared sensor based on ICT. Journal of Apiculture, 34, 47-55. https://doi.org/10.17519/apiculture.2019.04.34.1.47.
2. Kim JH, Seo H, Han W, Chung W (2021) A study on the honeycomb entry and exit counting system for measuring the amount of movement of honeybees inside the beehive. The Journal of the Convergence on Culture Technology, 7, 857-862. https://doi.org/10.17703/JCCT.2021.7.4.857.
3. Ngo TN, Wu KC, Yang EC, Lin TT (2019) A real-time imaging system for multiple honey bee tracking and activity monitoring. Computers and Electronics in Agriculture, 163, 104841. https://doi.org/10.1016/j.compag.2019.05.050.
4. Lei C, Lu Y, Xing Z, Zhang J, Li S, Wu W, Liu S (2024) A honey bee in-and-out counting method based on multiple object tracking algorithm. Insects, 15, 974. https://doi.org/10.3390/insects15120974.
5. Cecchi S, Spinsante S, Terenzi A, Orcioni S (2020) A smart sensor-based measurement system for advanced bee hive monitoring. Sensors, 20, 2726. https://doi.org/10.3390/s20092726.
6. Rigakis I, Potamitis I, Tatlas NA, Psirofonia G, Tzagaraki E, Alissandrakis E (2023) A low-cost, low-power, multisensory device and multivariable time series prediction for beehive health monitoring. Sensors, 23, 1407. https://doi.org/10.3390/s23031407.
7. Zaman A, Dorin A (2023) A framework for better sensor-based beehive health monitoring. Computers and Electronics in Agriculture, 210, 107906. https://doi.org/10.1016/j.compag.2023.107906.
8. Kwon KH, Cho C, Lee H (2019) Smart beehive using data fused preprocessing and artificial neural networks. Journal of Digital Contents Society, 20, 2321-2327. https://doi.org/10.9728/dcs.2019.20.12.2321.
9. Oh DG, Son MW, Akongte PN, Lee CH, Choi YS, Kim DW (2024) The effects of using heating panels in smart beekeeping systems on honeybee (*Apis mellifera*) colonies during winter: worker bee activity. Journal of Apiculture, 39, 1-10. https://doi.org/10.17519/apiculture.2024.04.39.1.1.
10. Kulyukin VA, Kulyukin AV (2023) Accuracy vs. energy: an assessment of bee object inference in videos from on-hive video loggers with YOLOv3, YOLOv4-Tiny, and YOLOv7-Tiny. Sensors, 23, 6791. https://doi.org/10.3390/s23156791.
11. Ju OJ, Soh H, Lee SW, Lee YS (2022) Climate-smart agriculture (CSA)-based assessment of a local rice cultivation in Hwaseong-city, Gyeonggi-do. Korean Journal of Environmental Agriculture, 41(1), 32-40. https://doi.org/10.5338/KJEA.2022.41.1.05.
12. Heo JW, Park KH, Lee JS, Hong SG, Lee GI, Baek JH (2018) Design of cloud-based data analysis system for culture medium management in smart greenhouses. Korean Journal of Environmental Agriculture, 37(4), 251-259. https://doi.org/10.5338/KJEA.2018.37.4.38.
13. Heo JW, Lee JS, Lee GI, Kim HH (2017) Growth of kale seedlings affected by the control of light quality and intensity under smart greenhouse conditions with artificial lights. Korean Journal of Environmental Agriculture, 36(3), 193-200. https://doi.org/10.5338/KJEA.2017.36.3.31.
14. Kim A, Kim B, Chon K, Lee H, Park YK, You AS, Park HH, Yun HJ (2020) Assessment of contact and oral toxicity of four neonicotinoid insecticides to bumblebees (*Bombus terrestris*). Korean Journal of Environmental Agriculture, 39(2), 106-113. https://doi.org/10.5338/KJEA.2020.39.2.14.
15. Lee SB, Oh YR, Song J, Kwak JH (2025) Performance measure of agricultural environment conservation program and suggestions. Korean Journal of Environmental Agriculture, 44, 188-199. https://doi.org/10.5338/KJEA.2025.44.20.
16. Lee HM, Kim HW, Kim JH, Kim MW (2024) Analysis of air pollutant characteristics in agricultural areas using continuous monitoring data. Korean Journal of Environmental Agriculture, 43, 200-210. https://doi.org/10.5338/KJEA.2024.43.19.
17. Yen TF, Oprea A, Onarlioglu K, Leetham T, Robertson W, Juels A, Kirda E (2013) Beehive: large-scale log analysis for detecting suspicious activity in enterprise networks. In: Proceedings of the 29th Annual Computer Security Applications Conference (ACSAC '13).

Association for Computing Machinery, New York, NY, USA, 199-208. https://doi.org/10.1145/2523649.2523670.
18. Hadjur H, Ammar D, Lefèvre L (2022) Toward an intelligent and efficient beehive: A survey of precision beekeeping systems and services. Computers and Electronics in Agriculture, 192, 106604. https://doi.org/10.1016/j.compag.2021.106604.
19. Abdollahi M, Giovenazzo P, Falk TH (2022) Automated beehive acoustics monitoring: A comprehensive review of the literature and recommendations for future work. Applied Sciences, 12(8), 3920. https://doi.org/10.3390/app12083920.
20. Šabić J, Perković T, Šolić P, Šerić L (2025) Buzzing with intelligence: A systematic review of smart beehive technologies. Sensors, 25(17), 5359. https://doi.org/10.3390/s25175359.
21. Meikle WG, Holst N (2015) Application of continuous monitoring of honeybee colonies. Apidologie, 46, 10-22. https://doi.org/10.1007/s13592-014-0298-x.
22. Meikle WG, Holst N, Colin T, Weiss M, Carroll MJ, McFrederick QS, Barron AB (2018) Using within-day hive weight changes to measure environmental effects on honey bee colonies. PLoS ONE, 13(5), e0197589. https://doi.org/10.1371/journal.pone.0197589.
23. Meikle WG, Rector BG, Mercadier G, Holst N (2008) Within-day variation in continuous hive weight data as a measure of honey bee colony activity. Apidologie, 39(6), 694-707. https://doi.org/10.1051/apido:2008055.
24. Henry E, Adamchuk V, Stanhope T, Buddle C (2019) Precision apiculture: development of a wireless sensor network for honeybee hives. Computers and Electronics in Agriculture, 156, 138-144. https://doi.org/10.1016/j.compag.2018.11.030.
25. Kviesis A, Zacepins A, Komasilovs V, Kviesis A (2023) Bee colony remote monitoring based on IoT using ESP-NOW protocol. PeerJ Computer Science, 9, e1363. https://doi.org/10.7717/peerj-cs.1363.
26. Tashakkori R, Hamza AS, Crawford MB (2021) Beemon: An IoT-based beehive monitoring system. Computers and Electronics in Agriculture, 190, 106427. https://doi.org/10.1016/j.compag.2021.106427.
27. Stabentheiner A, Kovac H, Mandl M, Käfer H (2021) Coping with the cold and fighting the heat: Thermal homeostasis of a superorganism, the honeybee colony. Journal of Comparative Physiology A, 207(3), 337-351. https://doi.org/10.1007/s00359-021-01464-8.
28. Jhawar J, Morris RG, Shukla A, Rangarajan G, Sinha S (2023) How honeybees respond to heat stress from the individual to colony level. Journal of the Royal Society Interface, 20, 20230290. https://doi.org/10.1098/rsif.2023.0290.